NASA TECHNICAL MEMORANDUM

NASA TM X-71932

COPY NO.

NASA TM X-71932

FREE-FLIGHT WIND-TUNNEL INVESTIGATION OF A FOUR-ENGINE SWEPTWING UPPER-SURFACE BLOWN TRANSPORT CONFIGURATION

By

Lysle P. Parlett

March 1974

NATIONAL AERONAUTICS AND SPACE ADMINISTRATION

LANGLEY RESEARCH CENTER, HAMPTON, VIRGINIA 23665

1. Report No.	2. Government Accession No.	3. Recipient's Catalog No.
NASA TM X-71932		

4. Title and Subtitle	5. Report Date
Free-Flight Wind-Tunnel Investigation of a Four-Engine Sweptwing Upper-Surface Blown Transport Configuration	March 1974
	6. Performing Organization Code: 35.210

7. Author(s)	8. Performing Organization Report No.
Lysle P. Parlett	

9. Performing Organization Name and Address	10. Work Unit No.
NASA Langley Research Center Hampton, Virginia 23665	760-61-02-01
	11. Contract or Grant No.

12. Sponsoring Agency Name and Address	13. Type of Report and Period Covered
NASA Langley Research Center Hampton, Virginia 23665	Interim/Feb. 1974
	14. Sponsoring Agency Code

15. Supplementary Notes

Interim technical information release, subject to possible revision and/or later formal publication

16. Abstract

The dynamic stability characteristics of a four-engine turbofan transport model having an upper-surface blown-jet flap have been investigated by means of the free-flight technique in the Langley full-scale tunnel. The flight characteristics of the model were investigated through a range of lift coefficients from 3 to 8 with all four engines operating and with one outboard engine not operating. Static characteristics were investigated by conventional power-on force tests over the flight-test angle-of-attack range and through the stall.

17. Key Words (Suggested by Author(s)) (STAR category underlined)	18. Distribution Statement
Aerodynamics, Powered Lift, Upper-Surface-Blown, Jet Flap, Fluid Mechanics, Dynamic Stability	No FEDD limitation Foreign distribution excluded

19. Security Classif. (of this report)	20. Security Classif. (of this page)	21. No. of Pages	22. Price*
Unclassified	Unclassified		$3.25

*Available from { The National Technical Information Service, Springfield, Virginia 22151
STIF/NASA Scientific and Technical Information Facility, P.O. Box 33, College Park, MD 20740

FREE-FLIGHT WIND-TUNNEL INVESTIGATION OF A FOUR-ENGINE SWEPTWING UPPER-SURFACE BLOWN TRANSPORT CONFIGURATION

By Lysle P. Parlett
Langley Research Center

SUMMARY

The stability and control characteristics of a four-engine sweptwing turbofan transport model having an upper-surface blown jet flap have been investigated by means of the free-flight technique in the Langley full-scale tunnel. The flight characteristics of the model were investigated under conditions of symmetric and asymmetric (one outboard engine inoperative) thrust at lift coefficients up to 8. Static characteristics were investigated by conventional power-on force tests over the flight-test angle-of-attack range and through the stall.

The results of the investigation showed that in either the four-engine condition, or with one outboard engine inoperative, longitudinal motions of the model were heavily damped over the test angle-of-attack range. The model was easy to fly, but the longitudinal control power became marginal at the highest lift coefficients because of reduced free-stream dynamic pressure. Laterally, the model was difficult to fly without artificial stabilization because of a lightly damped Dutch-roll oscillation which was easily excited by the use of rudder control. Adequate damping of the oscillation could be achieved, however, by the addition of artificial damping about the roll and yaw axes and, with this additional damping, the model was easy to fly. With one outboard engine inoperative, lateral trim could be restored by the use of asymmetric blowing, that is, by blowing on the wing leading edge and on the outboard segment of the full-span flap of the engine-out wing. In trimmed, three-engine flight, the stability and controllability of the model were not noticeably different from what they had been in four-engine operation.

INTRODUCTION

Previous static force test investigations have shown that configurations utilizing the upper-surface blown jet-flap concept can achieve the high-lift coefficients required for STOL operation, and acoustic studies have indicated that the shielding effect of the wing may substantially reduce the ground level noise associated with powered lift. (See refs. 1 and 2, respectively.) The present investigation was undertaken to probe, by means of the free-flight technique, the area of dynamic stability and control for problems which might not appear during the course of more conventional testing. Experience has shown the free-flight technique to be a valuable tool in

exploratory investigations on new types of aircraft, most notably in the VTOL and STOL fields where large power effects and stalled or near-stalled conditions have to be considered. In the present investigation, particular emphasis was placed on engine-out conditions (one outboard engine inoperative) in which, at high lift, the development and effects of asymmetric stall are difficult to predict, and where the effects of the lateral trim devices on dynamic stability were unknown.

The model used in the investigation was a four-engine configuration with pod-mounted fan engines located on top of the wing, close to the fuselage in a twin-engine (siamese) nacelle. The model was flown with flap deflections of 35° and 50° over a range of lift coefficients from 3 to 8 with all four engines running and with one engine inoperative. Supplementary static force tests were made to determine static stability characteristics of the flight-test model over the flight-test angle-of-attack range, and including the stall.

SYMBOLS

The longitudinal data are referred to the stability-axis system and the lateral data are referred to the body-axis system. (See fig. 1.) The origin of the axes was located to correspond to the center-of-gravity position (0.40 mean aerodynamic chord) shown in figure 2.

Measurements and calculations were made in the U.S. Customary Units and are presented in both the International System of Units (SI) and U.S. Customary Units. Equivalent dimensions were determined by using the conversion factors given in reference 3.

b	wing span, m (ft)
C_D	drag coefficient, $\frac{F_D}{q_\infty S}$
C_L	lift coefficient, $\frac{F_L}{q_\infty S}$
C_ℓ	rolling-moment coefficient, $\frac{M_X}{q_\infty S b}$
C_m	pitching-moment coefficient, $\frac{M_Y}{q_\infty S \bar{c}}$
C_n	yawing-moment coefficient, $\frac{M_Z}{q_\infty S b}$

C_Y	lateral force coefficient, $\frac{F_Y}{q_\infty S}$
C_μ	engine total gross-thrust coefficient, $\frac{T}{q_\infty S}$
$C_{\mu,ail}$	aileron blowing jet momentum coefficient, $\frac{R}{q_\infty S}$
$C_{\mu,ail,L}$	left aileron blowing jet momentum coefficient, $\frac{R}{q_\infty S}$
$C_{\mu,le}$	wing leading-edge blowing jet momentum coefficient, $\frac{R}{q_\infty S}$
$C_{\mu,le,L}$	wing semispan leading-edge blowing jet momentum coefficient, left wing only, $\frac{R}{q_\infty S}$
$C_{\mu,r}$	rudder blowing jet momentum coefficient, $\frac{R}{q_\infty S}$
c	local wing chord, m (ft)
$\bar{c}$	mean aerodynamic chord, m (ft)
F_D	drag force, N (lb)
F_L	lift force, N (lb)
F_Y	force along Y axis, N (lb)
I_X	moment of inertia about X-body axis, kg-m^2 (slug-ft^2)
I_{XZ}	product of inertia about X- and Z-body axes, kg-m^2 (slug-ft^2)
I_Y	moment of inertia about Y-body axis, kg-m^2 (slug-ft^2)
I_Z	moment of inertia about Z-body axis, kg-m^2 (slug-ft^2)
i_t	horizontal tail incidence angle, positive leading edge up, deg

M_X	rolling moment, m-N (ft-lb)
M_Y	pitching moment, m-N (ft-lb)
M_Z	yawing moment, m-N (ft-lb)
q_∞	free-stream dynamic pressure, $\frac{\rho V^2}{2}$, N/m^2 (lb/ft^2)
R	resultant force, N (lb)
S	wing area, m^2 (ft^2)
T	static thrust, N (lb)
V	free-stream velocity, m/sec (ft/sec)
X, Y, Z	body reference axes
X_s, Y_s, Z_s	stability reference axes
x, y	flap coordinates, m (ft)
α	angle of attack, deg
β	angle of sideslip, deg
δ_e	elevator deflection, positive when trailing edge is down
δ_f	deflection of rear element of trailing-edge flap (same as δ_{f3} in figure 2(b)), positive when trailing edge is down, deg
δ_j	jet deflection, positive downward, deg
δ_r	rudder deflection, positive when trailing edge is left, deg
δ_s	spoiler deflection, positive when trailing edge is up, deg
$\delta_{s,ib,R}$	deflection of right inboard spoiler (see fig. 2(c)), positive when trailing edge is up, deg
$\delta_{s,ob,R}$	deflection of right outboard spoiler (see fig. 2(c)), positive when trailing edge is up, deg
ρ	air density, kg/m^2 ($slugs/ft^2$)

ϕ bank angle, deg or radians

ψ angle of yaw, deg or radians

$C_{\ell_\beta} = \frac{\partial C_\ell}{\partial \beta}$, per deg

$C_{n_\beta} = \frac{\partial C_n}{\partial \beta}$, per deg

$C_{Y_\beta} = \frac{\partial C_Y}{\partial \beta}$, per deg

MODEL AND APPARATUS

Both the force and flight tests were conducted on the four-engine sweptwing transport model illustrated by the three-view drawing of figure 2(a). Additional dimensional characteristics of the model are given in table I. The model had the full-span leading-edge and trailing-edge flaps shown in figure 2(b). Coordinates for each element of the triple-slotted trailing-edge flap are given in table II in terms of local wing chord. In order to close the flap slots behind the engines and provide a smooth contour (a Coanda flap) for the exhaust jet to follow, a thin piece of sheetmetal was used to fair over the upper surface of the triple-slotted trailing-edge flaps in the area immediately behind the engines as shown in figures 2(a) and 2(c).

Figure 2(c) presents details of the engine nacelle arrangement used in the tests. The inside contours of the exhaust nozzles were shaped so that the centerline of the exhaust flow was deflected downward toward the top of the wing, and the sides of the nacelles were flared outward to maintain the proper exit area for the turbofan simulators being used. The exhaust nozzles were rectangular with a combined aspect ratio (width/height) of 7.2.

Longitudinal trim and control were provided by an all-movable horizontal tail which had a 17-percent chord leading-edge flap and an elevator which was set at a constant deflection of -50°. Lateral directional control was provided by a rudder and by conventional spoilers which extended from the outboard edge of the Coanda flaps to the tips of the wings.

Blowing systems, illustrated in figure 2(d), provided boundary-layer control, when desired, for horizontal tail leading edge, the elevator, the rudder, the wing leading edge, and for the outboard segment of trailing-edge flap which is referred to herein as the aileron. In each of these systems, compressed air flowed from tubes through a row of small, closely spaced holes, then through slots to form a fairly uniform sheet across the forward surface of the airfoil or control element.

All tests were made in the 9- by 18-m (30- by 60-ft) open-throat test section of the Langley full-scale tunnel. The static force tests were made with an internal strain-gage balance and a conventional sting which entered the rear of the fuselage. Photographs of the model in force-test and flight-test conditions are presented in figures 3(a) and 3(b), respectively. Corrections for flow angularity were applied, but the model was so small in proportion to the tunnel test section that no wall corrections were needed or applied.

TESTS AND PROCEDURES

Static Force Tests

In preparation for the tests, engine calibrations were made to determine gross thrust as a function of engine rotational speed in the static condition, with flaps off. The tests were then made by setting the engine speed to give the desired gross thrust and holding these settings constant through the ranges of angle of attack or sideslip. Tests in the past have shown that the gross thrust of these engines at a constant rotational speed is not affected significantly by forward speed for the forward speeds involved in the present tests.

A few flow survey measurements were made in the vicinity of the horizontal tail to determine downwash characteristics. The measurements were made with a vane which was free to pivot for alinement with the local flow. By means of a potentiometer attached to the vane, the flow angle was indicated on a voltmeter.

During the tests, six-component longitudinal and lateral force-test data were measured at flap deflections of 35° and 50° through an angle-of-attack range of from about -5° to 35° at engine gross-thrust coefficients up to 1.0 per engine for four-engine and three-engine operations. Tests were made at various incidences of the horizontal tail and for various amounts of blowing over the wing leading edge and the control surfaces. The jet momentum for each of the blown surfaces was evaluated by measuring the force produced by the jet in the wind-off condition. Tests to determine static lateral stability derivatives were made at sideslip angles of -5° and 5°. Wind-on tests were made at a free-stream dynamic pressure of 109 N/m^2 (2.2 lb/ft^2), which correspond to a velocity of 13.1 m/sec (43 ft/sec), and a Reynolds number of 0.41×10^6. This value of Reynolds number was approximately the same as that of the flight tests which varied from 0.24×10^6 to 0.56×10^6.

Free-Flight Tests

In the test setup for the free-flight tests (shown in fig. 4), the model was flown without restraint in the 9- by 18-m (30- by 60-ft) open-throat test section of the tunnel and was remotely controlled about all three axes by two

human pilots. One pilot, located in an enclosure at the rear of the test section, controlled the model about its roll and yaw axes while the second pilot, stationed at one side of the test section, controlled the model in pitch. The model thrust operator was stationed with the pitch pilot. Compressed air, electric power, and control signals were supplied to the model through a flexible trailing cable composed of electric wires and lightweight plastic tubes. The cable also incorporated a 0.32-cm (1/8-in.) steel cable (attached to the model) that passed through a pulley above the test section and was used to catch the model in the event of an uncontrollable motion or mechanical failure. The entire flight cable was kept slack during the flights by a safety cable operator using a high-speed pneumatic winch. Further discussion of the free-flight technique, including the reasons for dividing the piloting tasks, is given in reference 4.

Artificial damping was applied, when desired, by deflecting the appropriate control surfaces (spoiler or rudder) by means of pneumatic servos whose output was controlled by signals from rate sensitive gyroscopes. Control travels used in the flight tests were ±5° deflection of the horizontal tail, ±12° deflection of the rudder, and 60° deflection of the spoilers.

Free-flight investigations of the stability and control characteristics of the model were made for trailing-edge flap deflections of 35° and 50° at angles of attack of approximately 0° to 20°, thereby covering a lift-coefficient range from about 3 to 8 in both the four-engine and three-engine conditions.

FORCE TEST RESULTS

Longitudinal

The longitudinal characteristics of the model for flap deflections of 35° and 50° are presented in figure 5. The high-lift coefficients shown in these figures are representative of those which would be required to provide safety margins for STOL operation, but the pitching-moment data show that high lift may be accompanied by problems in the areas of longitudinal stability and trim. Increases in thrust produce large increases in diving moments, and for any level of thrust the static stability (about the $0.40\bar{c}$ station) is positive at low angles of attack (negative values of $dC_m/d\alpha$) but became neutral or negative through much of the higher angle-of-attack range up to the stall, where a pitchup develops. Stability would, of course, be improved by moving the moment reference forward, but the problem of trimming the diving moments would be aggravated.

The effects on longitudinal characteristics of applying symmetrical blowing boundary-layer control to the leading edge of the wing are presented in figure 6. Such boundary-layer control produces a substantial increase in maximum lift coefficient, extends the range of unstalled angle of attack, and reduces the severity of the post-stall pitchup.

A major cause of the low longitudinal stability is apparently the powerful downwash in the region of the horizontal tail. Information from flow surveys in this region is summarized in figure 7 in terms of the variation of downwash factor $1 - \frac{\partial \varepsilon}{\partial \alpha}$ with thrust coefficient for two vertical locations of the horizontal tail. The higher location $\left(\frac{z}{\bar{c}} = 1.38\right)$ is the one used for all model force and flight tests. Figure 7 shows that at low engine thrust a tail at this location would be operating at a downwash factor of about 0.5 (approximately normal for conventional configurations) and that its effectiveness deteriorates somewhat as thrust increases. A tail at the lower location would probably be far less effective throughout the thrust range.

Lateral

Static lateral stability derivatives, presented in figure 8, show that the model is directionally stable (positive C_{n_β}) and has a large positive dihedral effect (negative C_{ℓ_β}). The effects of increasing engine thrust are negligible at low angles of attack but, at angles of attack above 10°, increasing thrust produces marked increases in both directional stability and dihedral effect.

The data of figures 9 to 12 show that the lateral moments which are produced by the failure of one outboard engine are large but can be trimmed out without any appreciable lift penalty by the use of asymmetric boundary-layer control on the wing leading edge and aileron of the engine-out wing. Engine-out basic data are presented in figure 9, and control data are presented in figures 10 and 11. Data from figures 9 and 10 are summarized in figure 12 as plots of rolling- and yawing-moment coefficients against lift coefficients for a configuration having a four-engine thrust-weight ratio of 0.6. In four-engine operation, the rolling (and yawing) moments would, of course, be zero and a maximum lift coefficient of approximately 10 could reasonably be expected. With the failure of one outboard engine, the thrust-weight ratio would fall to 0.45 and the maximum lift coefficient would become about 8, approximately what it would be in four-engine operation at three-quarters thrust, but the out-of-trim moments would be very large. Figure 12 shows that these moments can, however, be trimmed out by applying blowing boundary-layer control to the aileron and leading edge of the wing on the failed-engine side and that the maximum lift coefficient in the trimmed condition is as high as it was before the boundary-layer control was applied. It is important to note that the use of boundary-layer control to achieve roll trim also provides yaw trim for the engine-out condition in this particular case. The restoration of trim by the use of only boundary-layer control implies, of course, that the full effectiveness of the spoiler and rudder would still be available for lateral maneuver control.

FLIGHT TEST RESULTS

Longitudinal

The model was flown over a range of lift coefficients from 3 to 8 without longitudinal artificial stabilization, at flap deflections of 35° and 50°, in four-engine and three-engine conditions.

Through the lift coefficient range from 3 to approximately 6.5, the model was fairly easy to fly in pitch. The pitch response of the model following a 5° deflection of the horizontal tail was sluggish, but the pitch control was considered adequate for maneuvering the model within the test section and for overcoming random disturbances in the tunnel airstream. The pitching motions were well damped apparently because of the high values of pitch damping associated with jet flap configurations. (See ref. 5.) This high pitch damping also contributed to controllable flight conditions even at lift coefficients near 8 where force tests (see fig. 5) indicate negative static stability. These high values of pitch damping together with the high pitch inertia are the factors mainly responsible for the sluggish control response, but it should be noted that these factors also made the model insensitive to gust disturbances and helped to maintain steady flights for prolonged periods, with very little pilot effort, once a trim condition had been established.

As lift coefficient was increased above approximately 6.5, control power deteriorated due to reduced free-stream velocities until at the lift coefficient of 8 the control was so weak that response was extremely sluggish and recovery from a longitudinal disturbance became uncertain.

Boundary-layer control in the form of blowing over the leading edge of the horizontal tail and over the elevator was employed during all flights as a precaution against tail stall. The use of this boundary-layer control on the horizontal tail of the model does not necessarily imply that it would be required on a full-scale airplane because, at the low Reynolds numbers inherent in the model tests, stall occurs at a lower angle of attack than at full scale, and the use of boundary-layer control might be regarded as simply offsetting the adverse effects of low Reynolds number.

No change in longitudinal characteristics was noted when flights were performed with one outboard engine not operating. As in four-engine operation, the only problem was one of weak control at high lift.

Lateral

The most obvious lateral characteristics of the model were a very lightly damped Dutch roll oscillation and, at the highest lift coefficients, low control power. The Dutch roll appeared at all lift coefficients, and was easily excited by the use of rudder control. At lift coefficients below about 6.5, the deflection of a spoiler alone would produce rolling and yawing

moments in very nearly the correct combination for coordinated lateral control; addition of rudder deflection to the control system would then induce excessive favorable yaw and, thus, excite the oscillation. Regardless of the source of lateral control, the oscillation, once developed, produced an almost unflyable condition at any lift coefficient.

The Dutch roll oscillation was adequately damped by the addition of artificial damping about the roll and yaw axes. With the artificial damping, the model became dynamically stable and could be flown smoothly for long periods of time at any of the several lift coefficients at which flights were attempted in the range from 3 to 8.

Weak lateral control power became a problem at lift coefficients of 6.5 or over. At these lift coefficients, the favorable yaw effect of spoiler deflection became so weak that rudder deflection (unnecessary at low C_L's) was required in conjunction with spoiler deflection for controlling the model.

In engine-out operation (one outboard engine not operating), lateral trim was achieved by the simultaneous use of blowing boundary-layer control over the aileron and the leading edge of the wing on the failed engine side. With roll and yaw trim achieved in this manner and with artificial damping about the lateral axes, the model was flown successfully at several lift coefficients from 3 to 8. The dynamic lateral characteristics were found to be unaffected by the sources of lateral trim and the flight behavior was the same as it had been during four-engine operation.

SUMMARY OF RESULTS

A free-flight investigation of the dynamic stability characteristics of an upper-surface blown jet-flap transport model in landing configurations has yielded the following results.

1. Longitudinal motions were heavily damped over the test angle-of-attack range. The model was easy to fly up to a lift coefficient of about 6.5, but the longitudinal control became marginal at higher lift coefficients because of the reduced free-stream dynamic pressures.

2. Laterally, the model was difficult to fly without artificial stabilization because of a lightly damped Dutch-roll oscillation which was easily excited by the use of rudder control. Adequate damping of the oscillation could be achieved, however, by the addition of artificial stabilization about the roll and yaw axes.

3. In trimmed, three-engine flight, the dynamic behavior of the model was not noticeably different from that for four-engine operation.

REFERENCES

1. Phelps, Arthur E.; and Smith, Charles C., Jr.: Wind-Tunnel Investigation of an Upper Surface Blown Jet-Flap Powered-Lift Configuration. NASA TN D-7399, 1973.

2. Smith, Charles C., Jr.; and Phelps, Arthur E., III: Large-Scale Wind-Tunnel Investigation of a Semispan Model With an Unswept Wing and an Upper Surface Blown Jet Flap. NASA TN D-7526, Sept. 1973.

3. Mechtly, E. A.: The International Systems of Units - Physical Constants and Conversion Factors (Rev.). NASA SP-7012, 1969.

4. Parlett, Lysle P.; and Kirby, Robert H.: Test Techniques Used by NASA for Investigating Dynamic Stability Characteristics of V/STOL Models. AIAA Aerodynamic Testing Conference, March 1964, pp. 42-49.

5. Grafton, Sue B.; Parlett, Lysle P.; and Smith, Charles C., Jr.: Dynamic Stability Derivatives of a Jet Transport Configuration With High Thrust-Weight Ratio and an Externally Blown Jet Flap. NASA TN D-6440, 1971.

TABLE I.- MASS AND DIMENSIONAL CHARACTERISTICS OF MODEL

Weight, N (lb)	817 (183.5)
Moment of inertia:	
I_X, kg-m^2 (slug-ft^2)	25.9 (19.1)
I_Y, kg-m^2 (slug-ft^2)	42.3 (31.2)
I_Z, kg-m^2 (slug-ft^2)	61.9 (45.6)
I_{XZ}, kg-m^2 (slug-ft^2)	14.1 (10.4)
Fuselage:	
Length, cm (in.)	307 (121)
Wing:	
Area, m^2 (ft^2)	1.28 (13.7)
Span, cm (in.)	307 (121)
Aspect ratio	7.5
Mean aerodynamic chord, cm (in.)	45.4 (17.9)
Spanwise location of mean aerodynamic chord, cm (in.)	62.3 (24.5)
Tip chord, cm (in.)	20.4 (8.04)
Root chord, cm (in.)	62.2 (24.5)
Sweep of quarter-chord line, deg	24
Dihedral of quarter-chord line, deg	-3.5
Engines:	
Spanwise location of inboard engines, cm (in.)	31.1 (12.3)
Spanwise location of outboard engines, cm (in.)	50.8 (20.0)
Exit area (per engine), m^2 (ft^2)	0.0159 (0.172)
Vertical tail:	
Span, cm (in.)	61.0 (24.0)
Root chord, cm (in.)	47.3 (18.6)
Tip chord, cm (in.)	32.1 (12.6)
Area, m^2 (ft^2)	0.242 (2.60)
Sweep of quarter-chord line, deg	35
Horizontal tail:	
Span, cm (in.)	152.0 (59.9)
Root chord, cm (in.)	42.1 (16.6)
Tip chord, cm (in.)	15.6 (6.14)
Area, m^2 (ft^2)	0.437 (4.71)
Sweep of quarter-chord line, deg	25

TABLE I.- MASS AND DIMENSIONAL CHARACTERISTICS OF MODEL - Concluded

Control surface dimensions

Rudder:	
Span, cm (in.)	55.8 (22.0)
Chord, inboard end, cm (in.)	16.8 (6.62)
Chord, outboard end, cm (in.)	12.5 (4.92)
Hinge-line location, percent chord	55
Sweep of hinge line, deg	34
Elevator:	
Span, cm (in.)	53.7 (21.2)
Chord, inboard end, cm (in.)	11.0 (4.33)
Chord, outboard end, cm (in.)	5.5 (2.17)
Hinge line location, percent chord	73
Sweep of hinge line, deg	17
Aileron:	
Span, cm (in.)	37.8 (14.9)
Chord, inboard end, cm (in.)	73.2 (28.9)
Chord, outboard end, cm (in.)	4.6 (1.81)
Spoiler:	
Span, cm (in.)	93.4 (36.8)
Chord, inboard end, cm (in.)	6.45 (2.00)
Chord, outboard end, cm (in.)	2.24 (0.87)

TABLE II.- FLAP COORDINATES

[Coordinates are given as percent of local wing chord]

First Element

x	y_{upper}	y_{lower}
0.00	1.67	1.67
1.39	4.33	.11
2.78	5.67	.00
4.17	6.44	
5.56	6.83	
6.44	6.83	
8.33	6.67	
9.72	6.28	
11.11	5.94	
12.50	5.56	
13.61	5.11	
15.28	4.61	1.50
16.67	4.06	2.39
18.06	3.61	3.00
19.17	3.22	3.17

Second Element

x	y_{upper}	y_{lower}
0.00	0.94	0.94
.94	2.39	.11
1.78	2.67	.00
2.78	2.94	.17
3.72	3.06	.39
4.61	2.94	.56
5.56	2.83	.72
6.50	2.61	.94
7.06	2.39	.94
7.39	2.22	.94
8.33	1.78	.72
9.28	1.27	.56
10.17	.72	.28
11.00	.11	.00

Third Element

x	y_{upper}	y_{lower}
0.00	0.72	0.72
.72	2.50	.11
1.83	3.17	.06
2.78	3.44	.00
3.72	3.50	
4.44	3.50	
5.56	3.50	
7.39	3.33	
9.28	3.06	
11.11	2.78	.06
12.94	2.39	.11
14.83	2.11	.17
16.67	1.83	.17
18.50	1.56	.17
20.39	1.22	.17
22.22	.83	.11
24.06	.56	.06
24.94	.28	.00

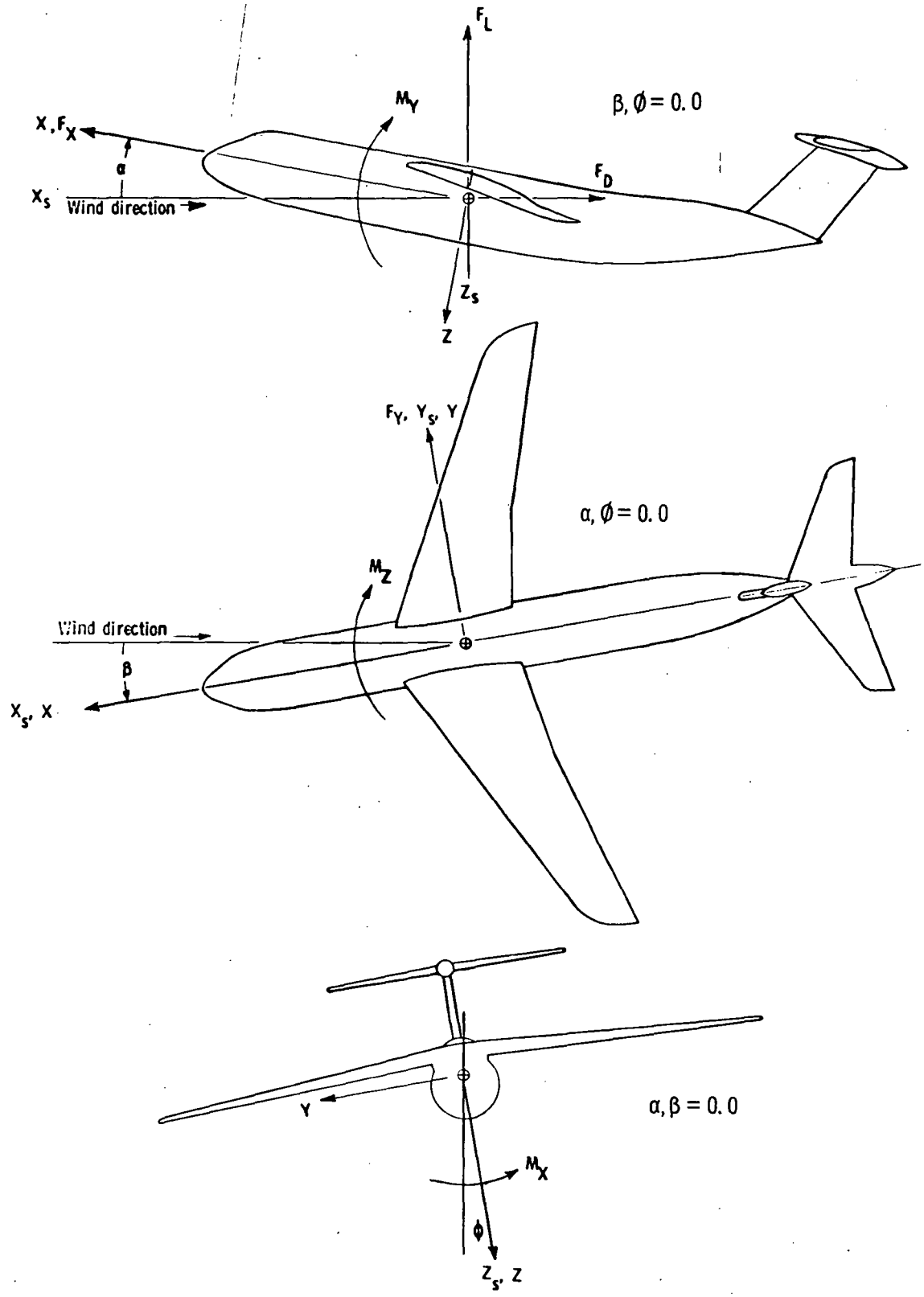

Figure 1. - Axis system used in presentation of results. Arrows indicate positive direction of moments, axis directions, and angles.

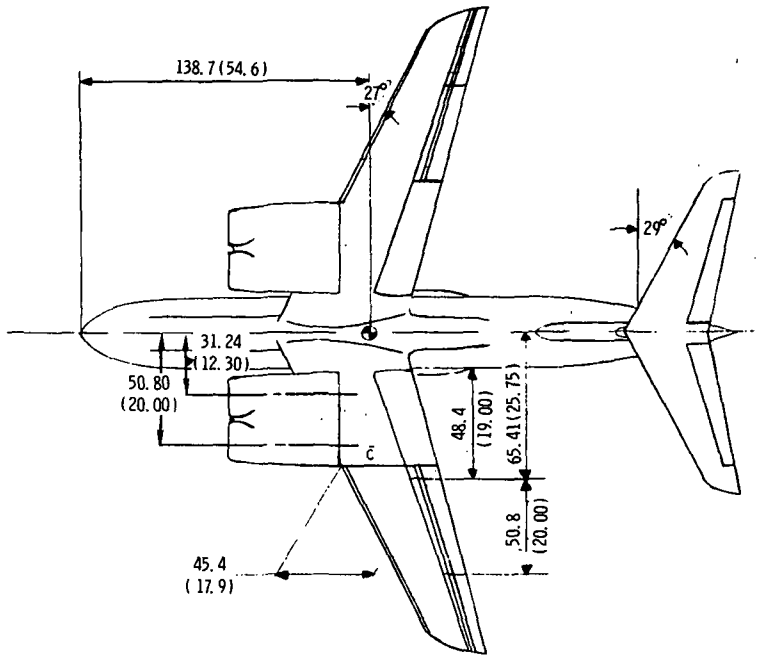

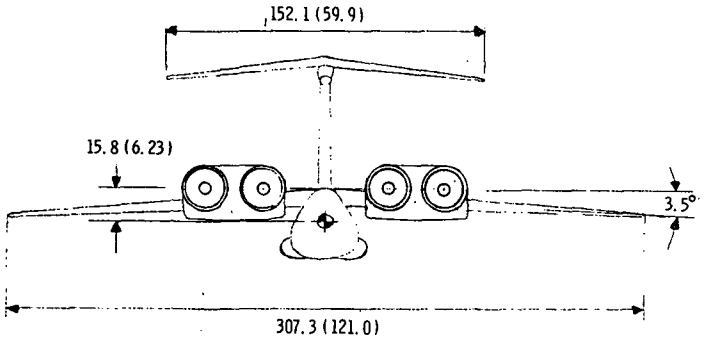

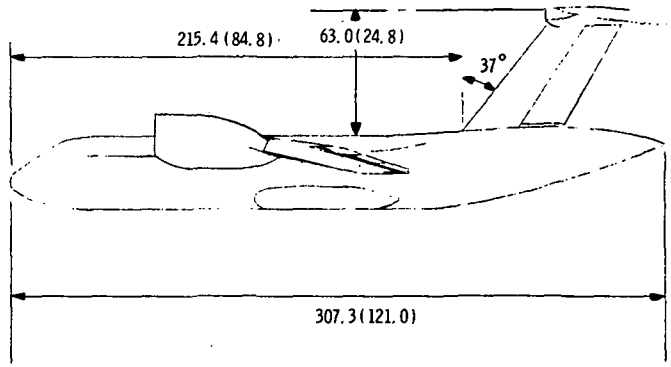

(a) Three-view drawing of complete model.

Figure 2. - Drawings of model used in investigation. All dimensions are in centimeters (inches).

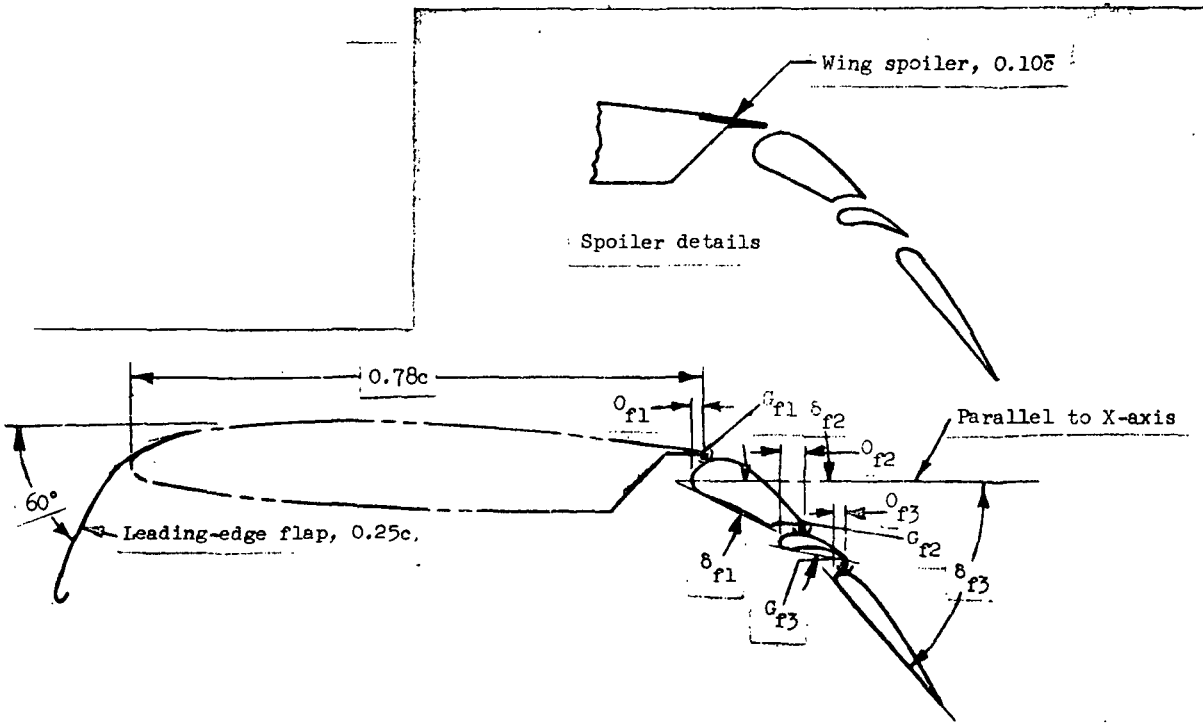

	A, cm (in.)	B, cm (in.)
Inboard	1.91 (0.75)	13.25 (5.22)
Outboard	12.20 (4.81)	14.00 (5.50)

δ_{f1}, deg	δ_{f2}, deg	δ_{f3}, deg	Overlap 1, O_{f1} percent c	Gap 1, G_{f1} percent c	Overlap 2, O_{f2} percent c	Gap 2, G_{f2} percent c	Overlap 3, O_{f3} percent c	Gap 3, G_{f3} percent c
25.0	10.0	35.0, 50.0,	1.47	1.61	3.98	1.61	1.39	1.61

(b) Flap assembly details.

(See table II for flap coordinates).

Figure 2. - Continued.

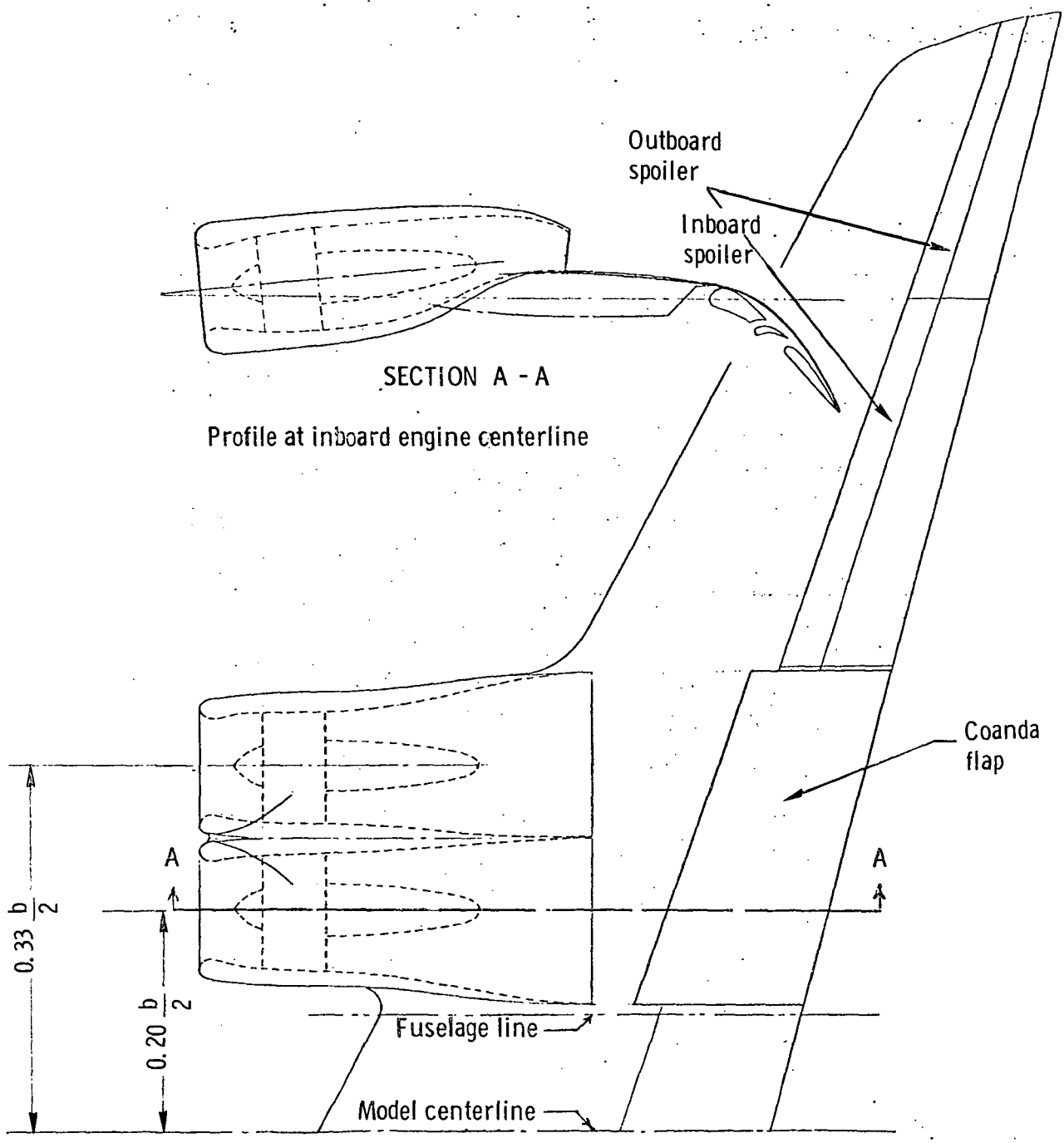

(c) Details of nacelle and Coanda flap.

Figure 2. - Continued.

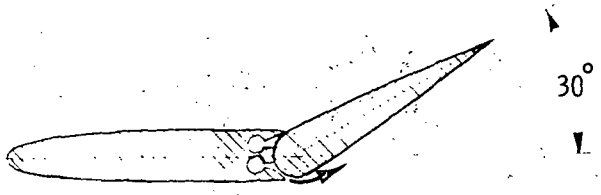

Cross section of vertical tail

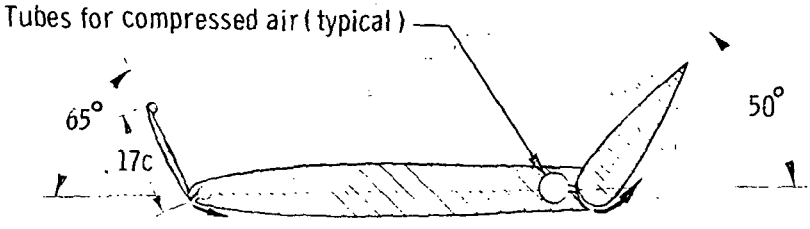

Cross section of horizontal tail

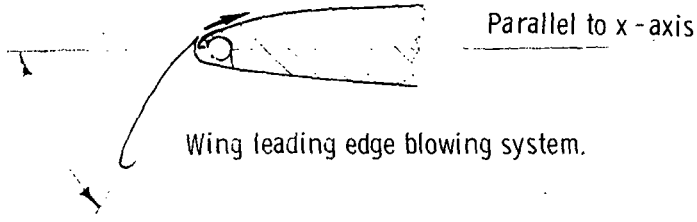

Wing leading edge blowing system.

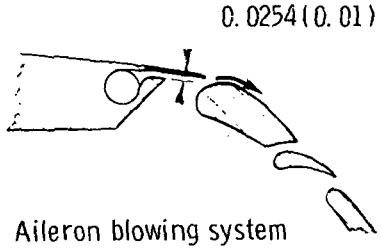

Aileron blowing system
(Outboard flap segment)

(d) Details of boundary-layer control system.

Figure 2. - Concluded.

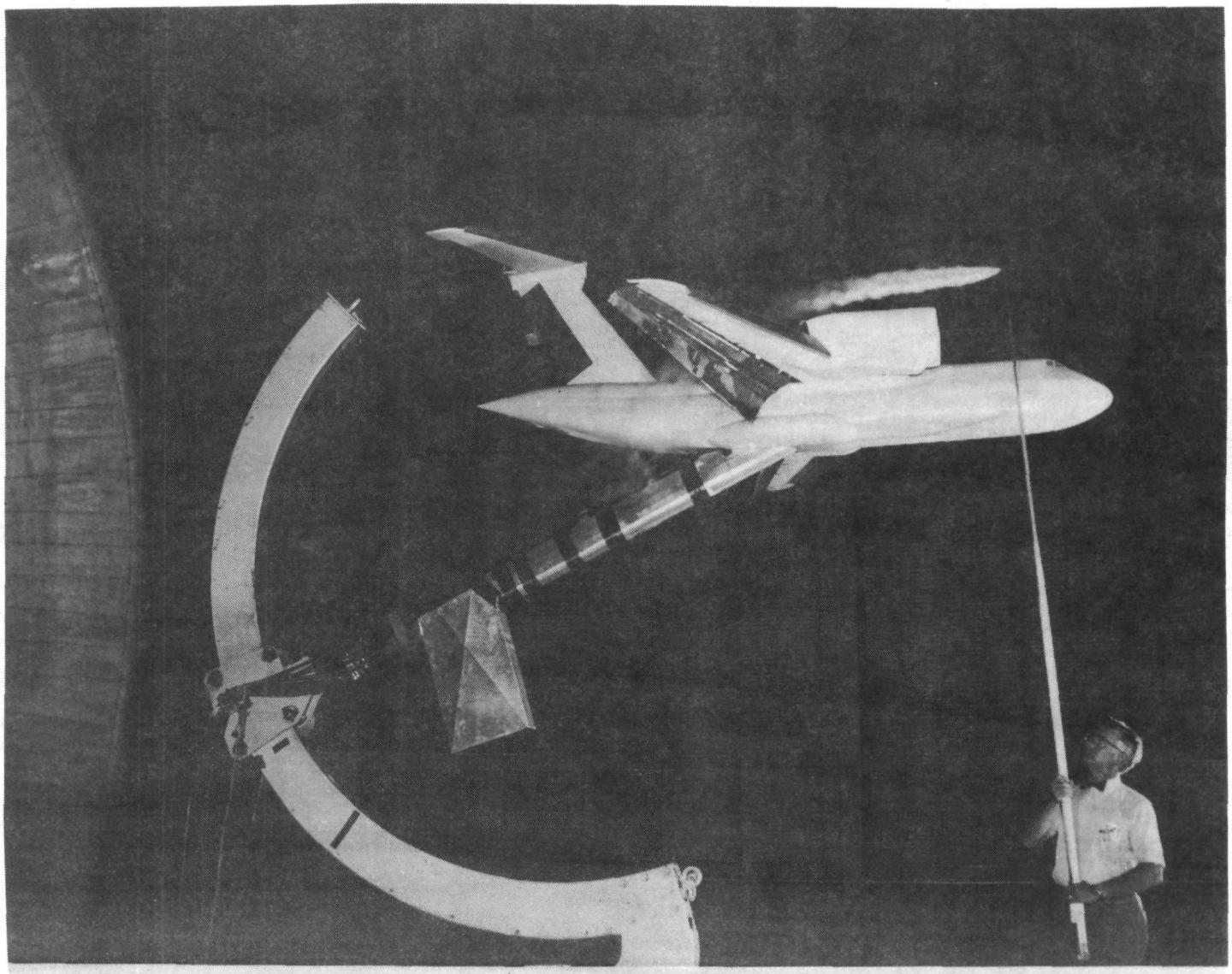

(a) Mounted for force tests, undergoing smoke flow studies.

Figure 3. - Photographs of model.

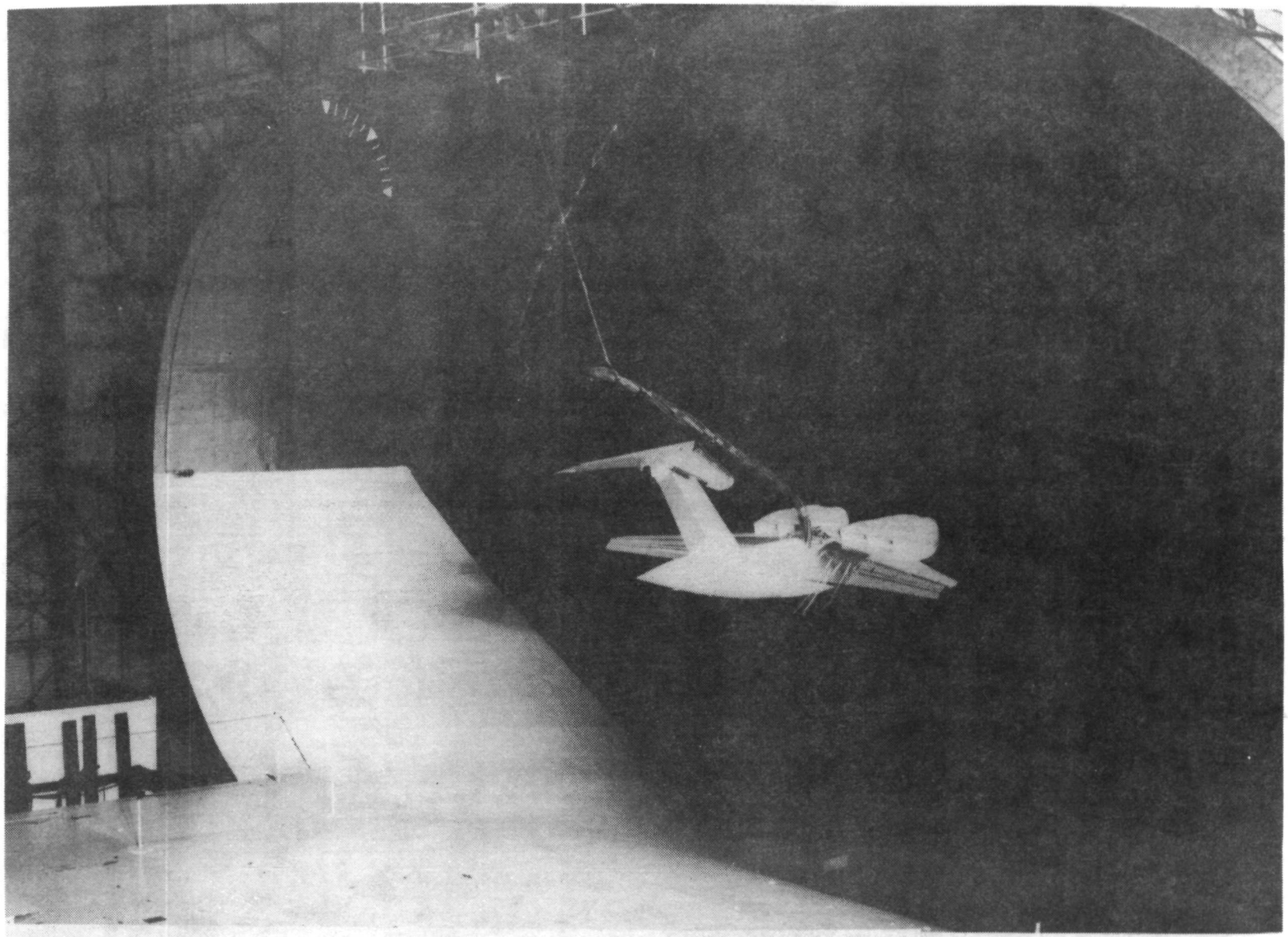

(b) Flying in tunnel.

Figure 3. - Concluded.

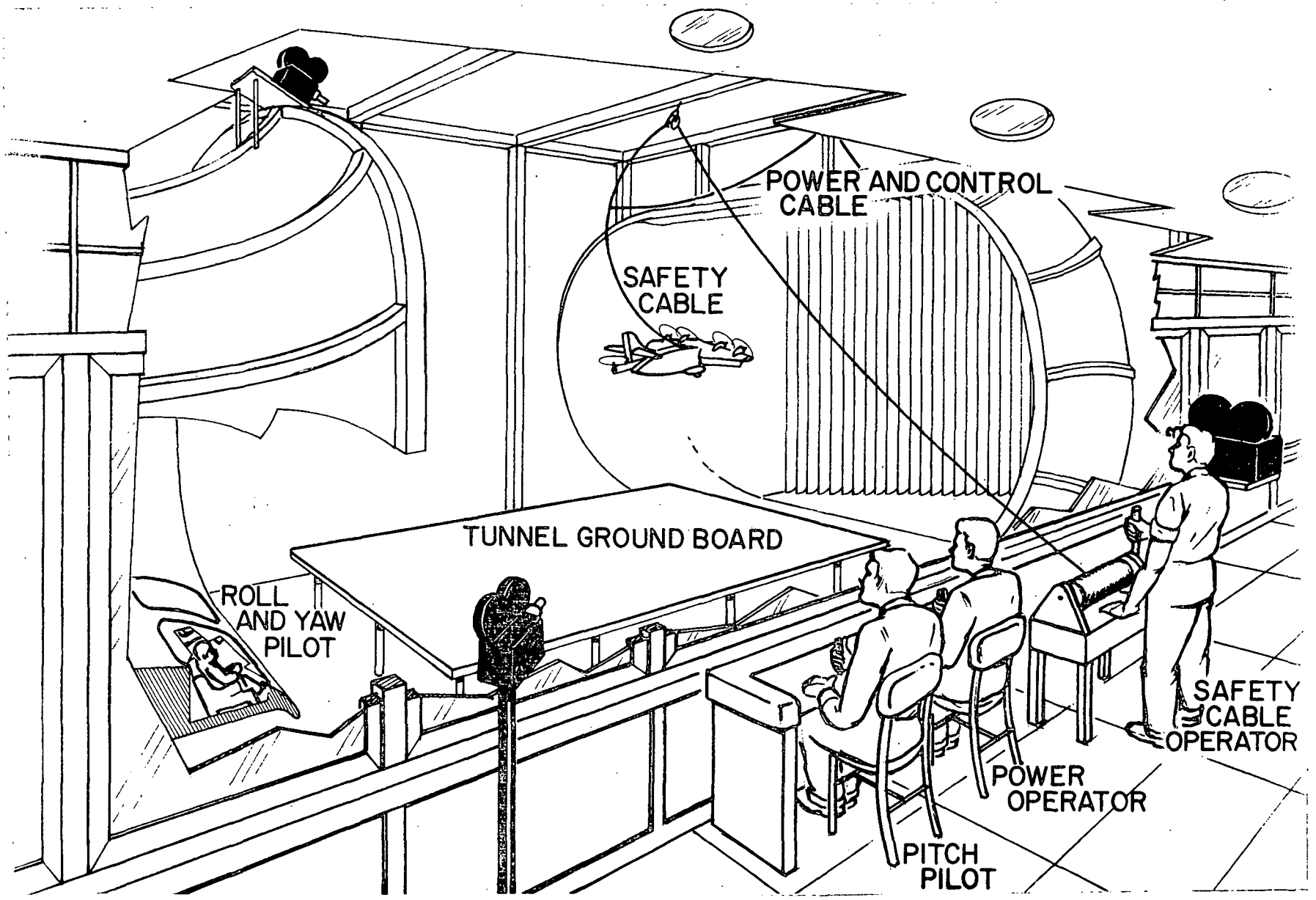

Figure 4. - Test set-up for free-flight model testing in Langley full-scale tunnel.

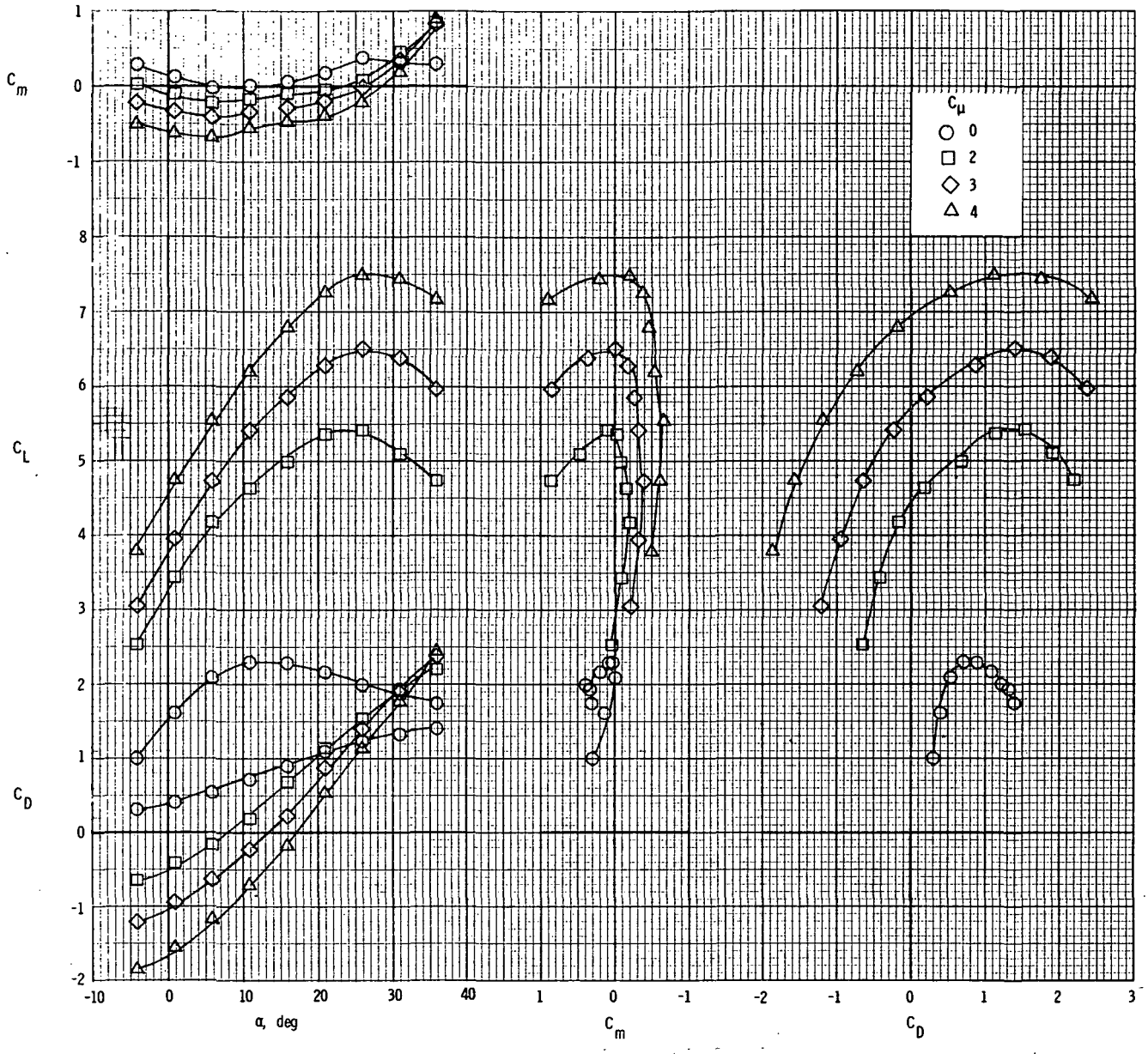

(a) $\delta_f = 35°$; $i_t = 5°$.

Figure 5. - Longitudinal characteristics, all engines operating.

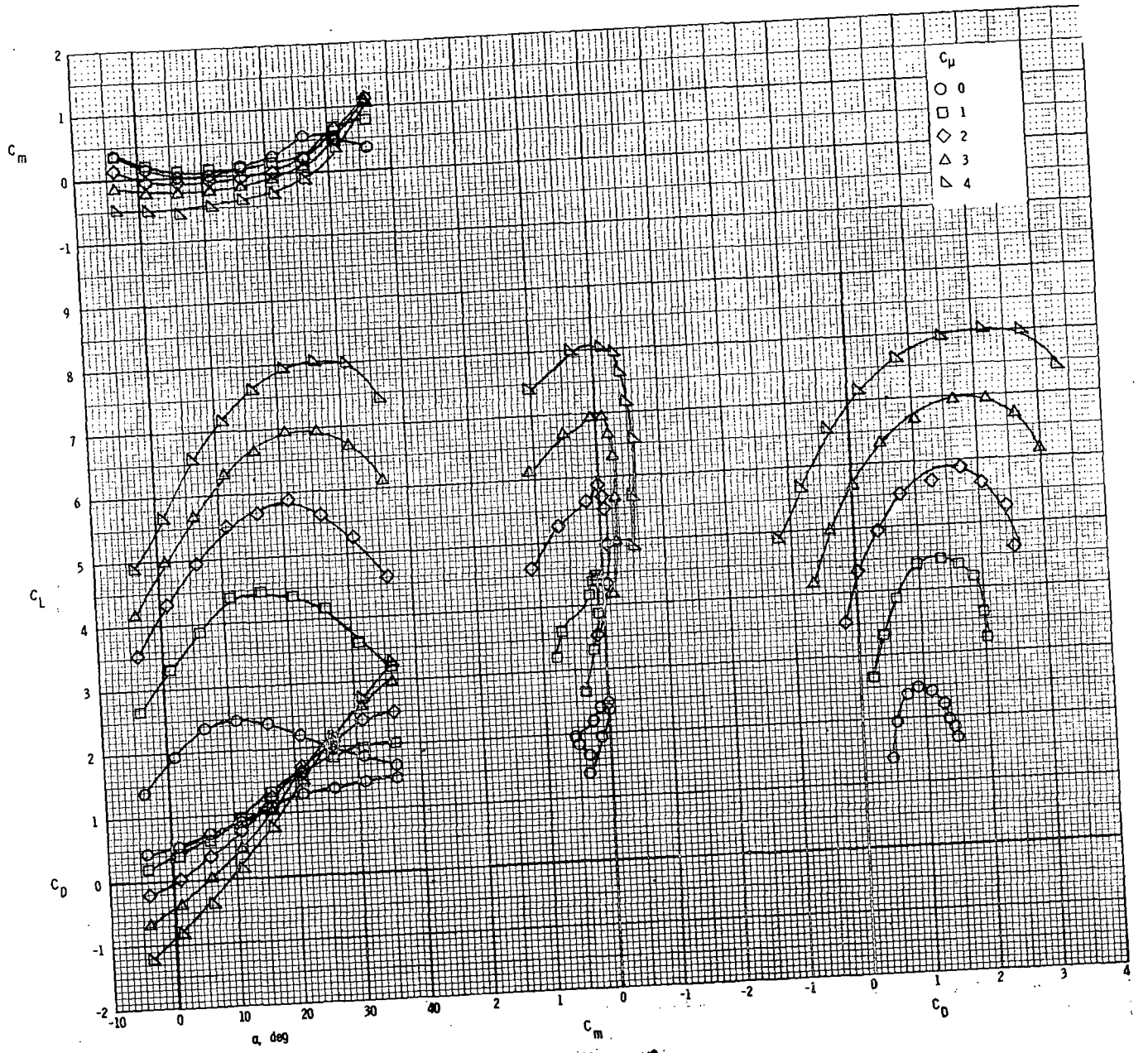

(b) $\delta_f = 50°$; $i_t = 6.5°$.

Figure 5. - Concluded.

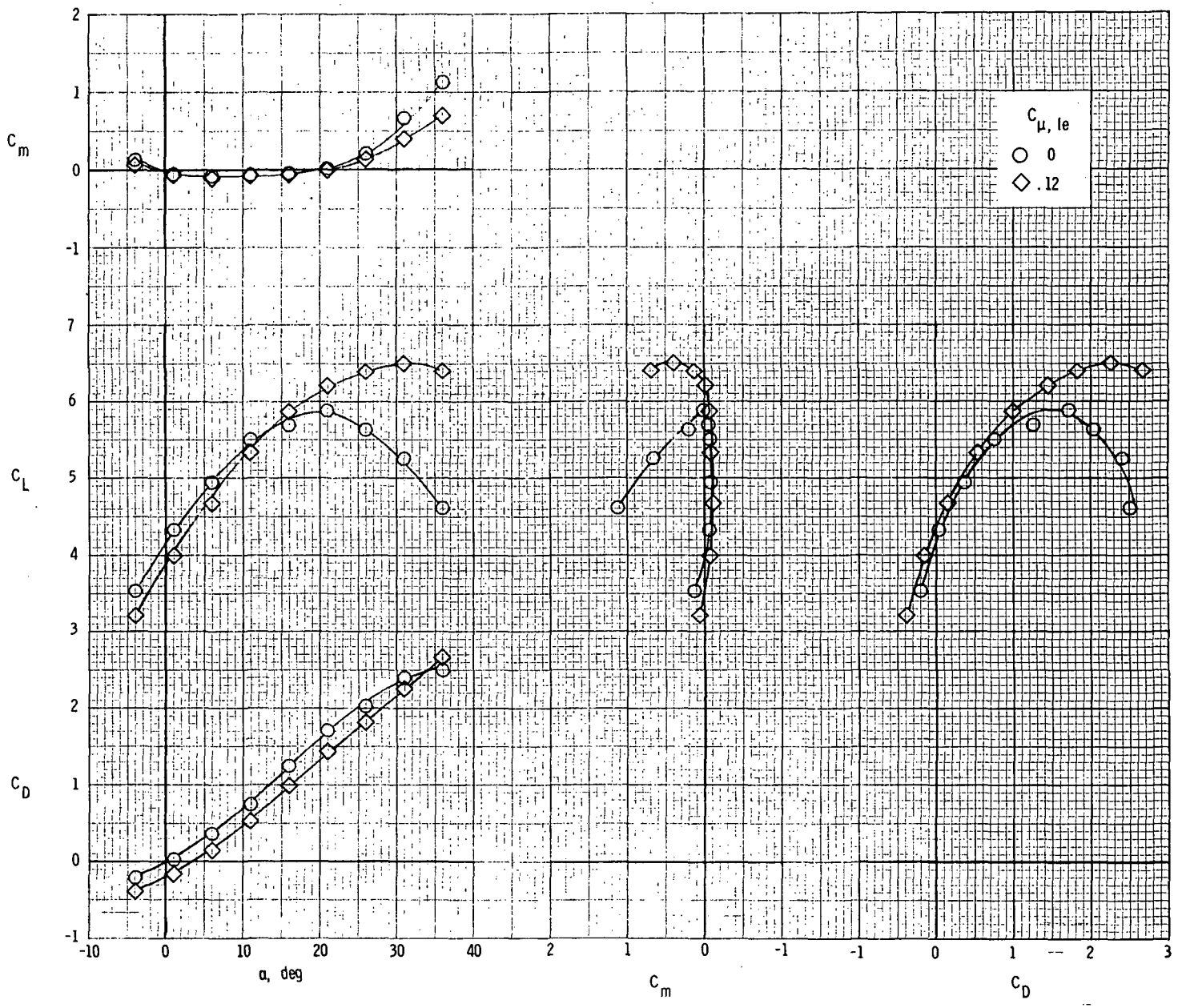

Figure 6. - Effect of blowing boundary-layer control on longitudinal characteristics.
$C_{\mu} = 2.0$; $\delta_f = 50^{\circ}$.

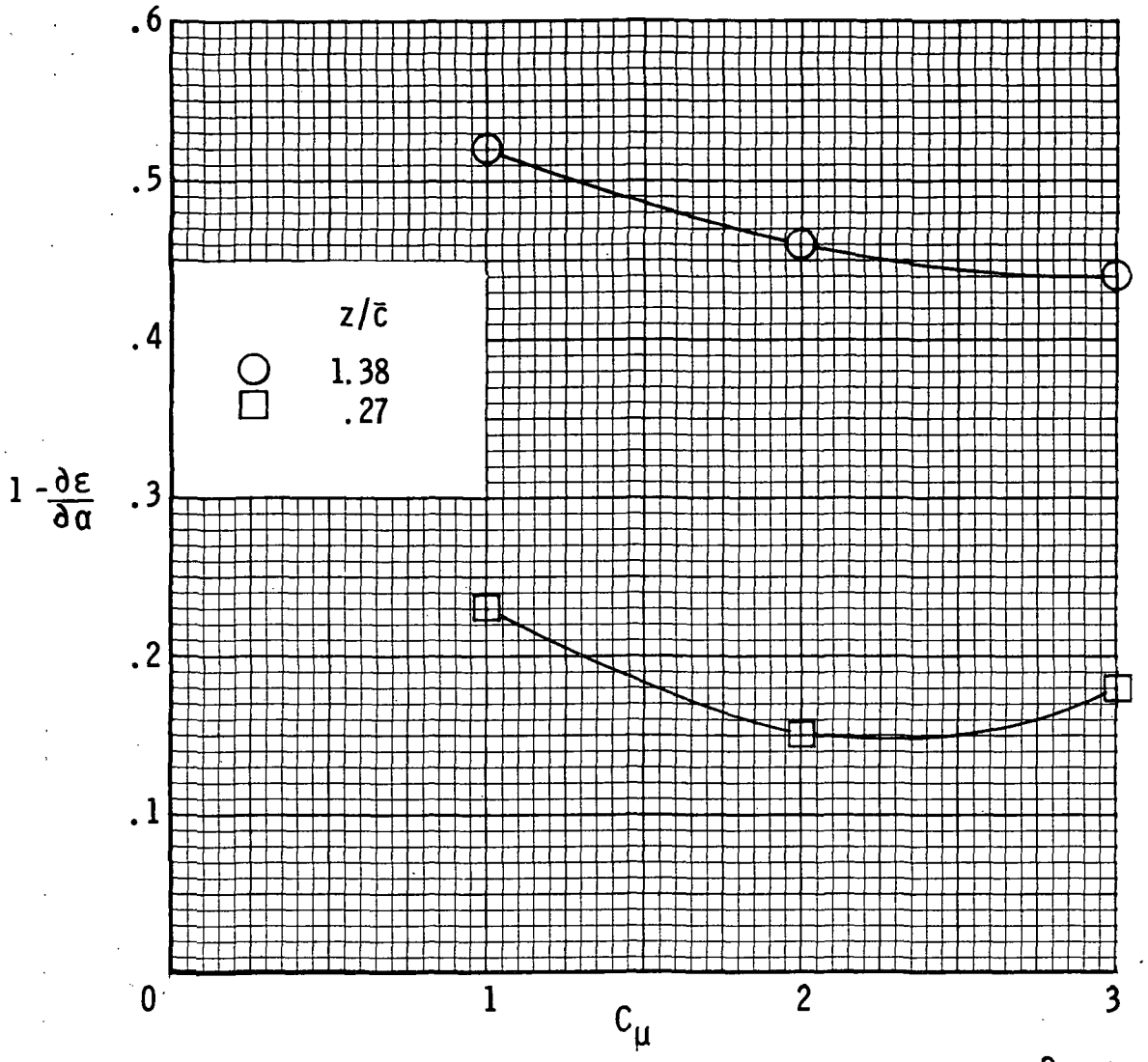

Figure 7. - Effect of tail height on average down wash factor at tail. $\delta_f = 50°$, $x/\bar{c} = 3.10$.

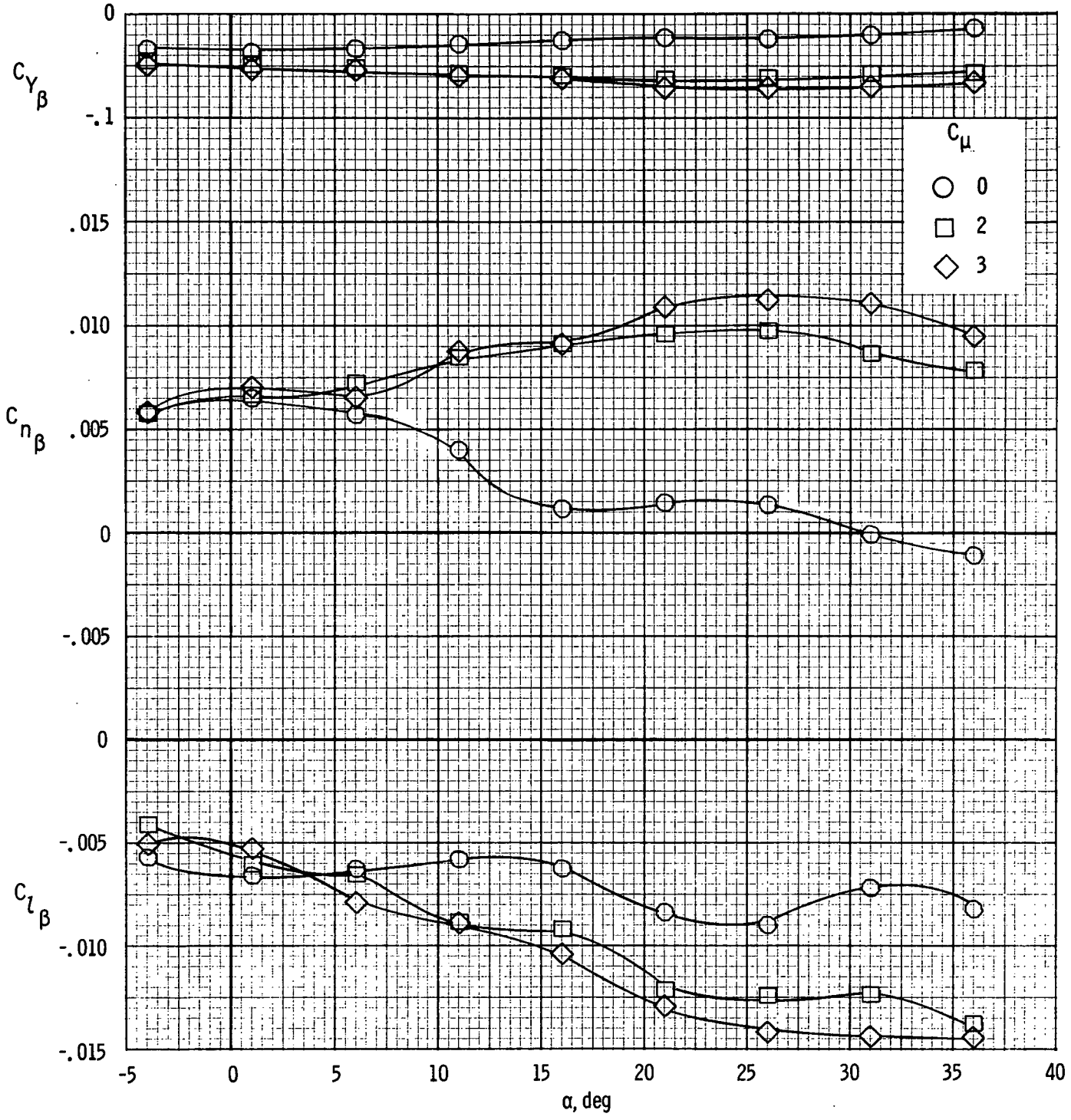

Figure 8. - Lateral static stability characteristics. $\delta_f = 50°$; $i_t = 5°$.

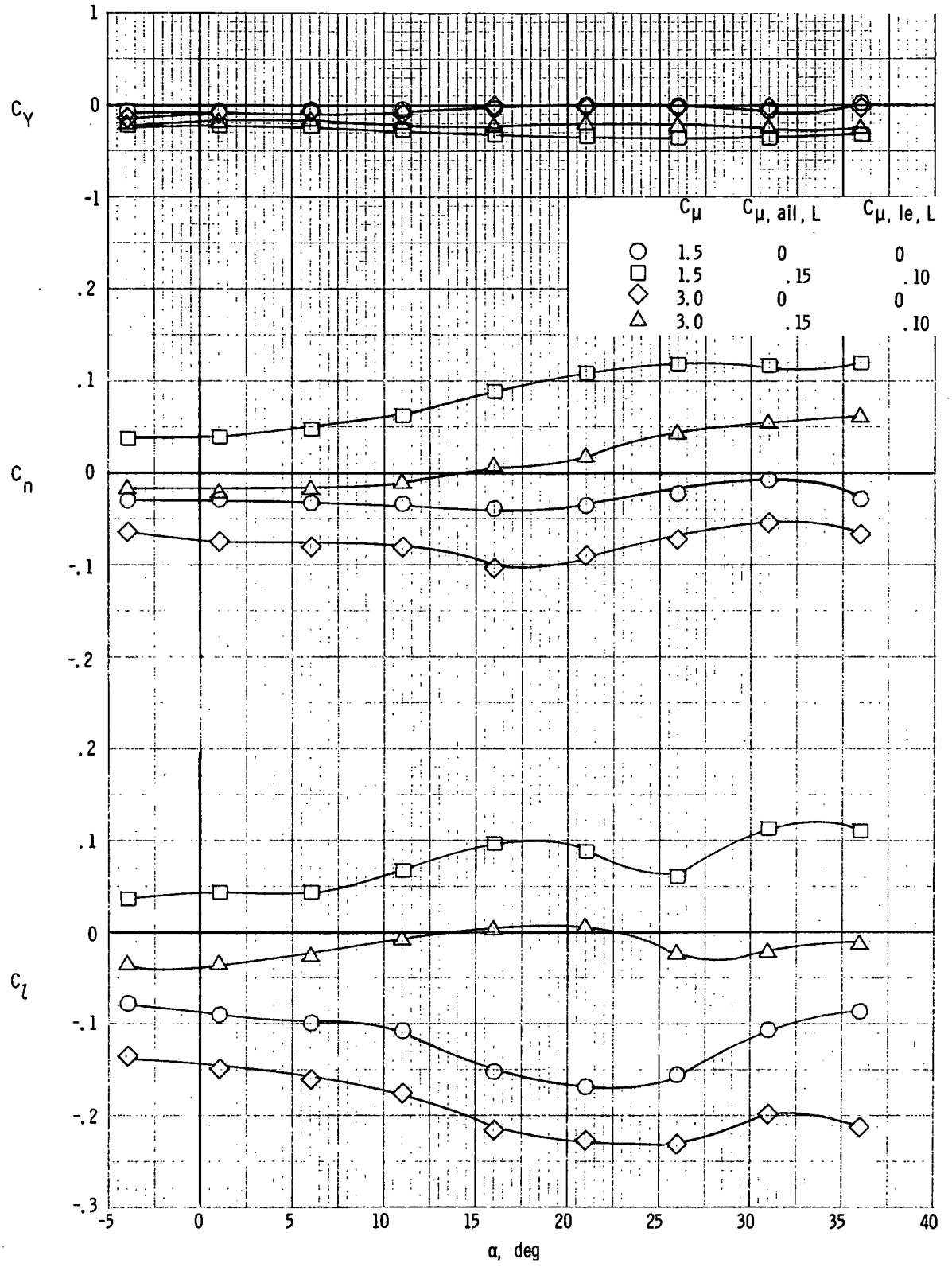

(a) Lateral characteristics.

Figure 9. - Effect of asymmetric blowing boundary-layer control on lateral characteristics. Left outboard engine not operating. $\delta_f = 50°$; $i_t = 5°$.

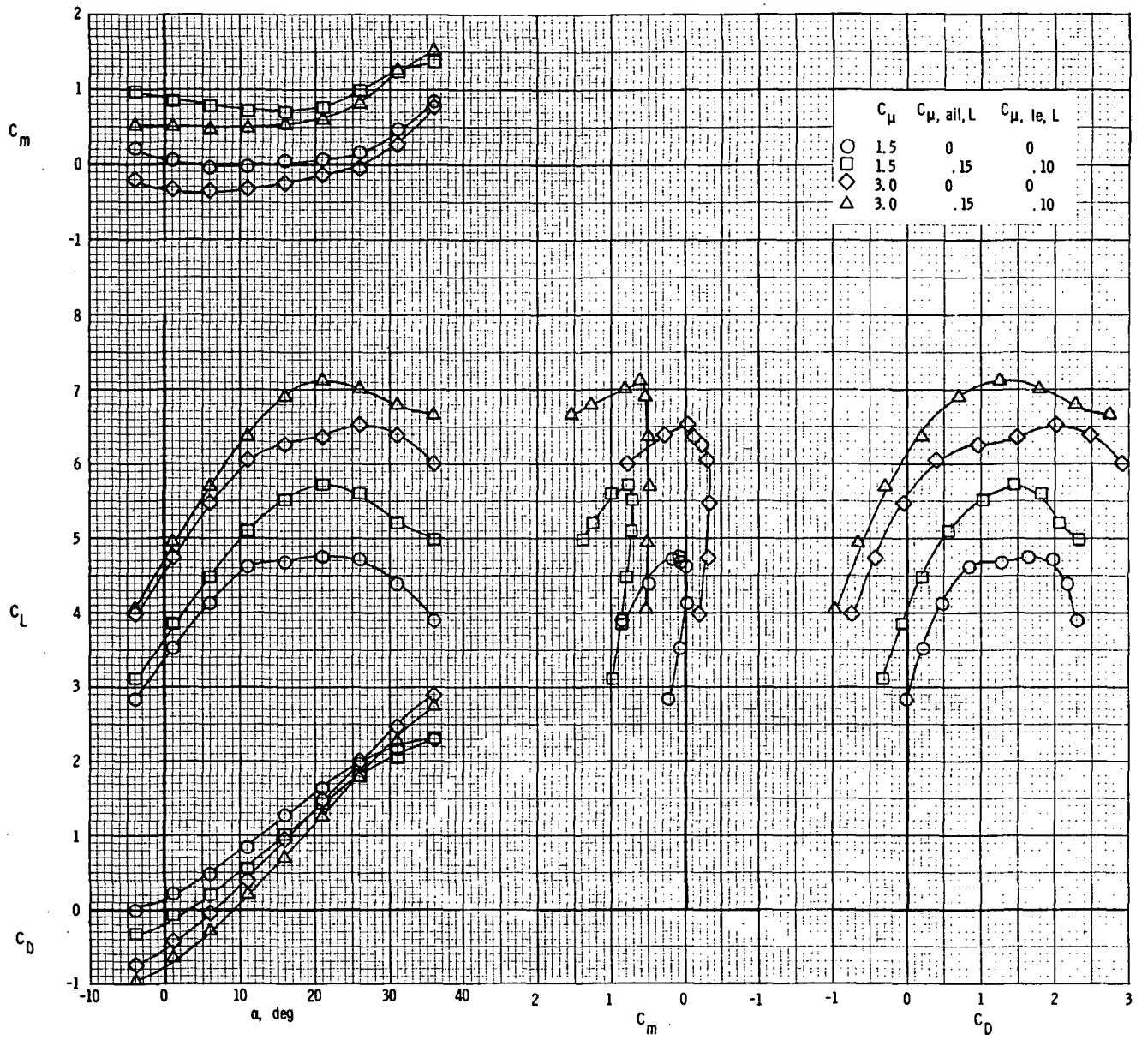

(b) Longitudinal characteristics.

Figure 9. - Concluded.

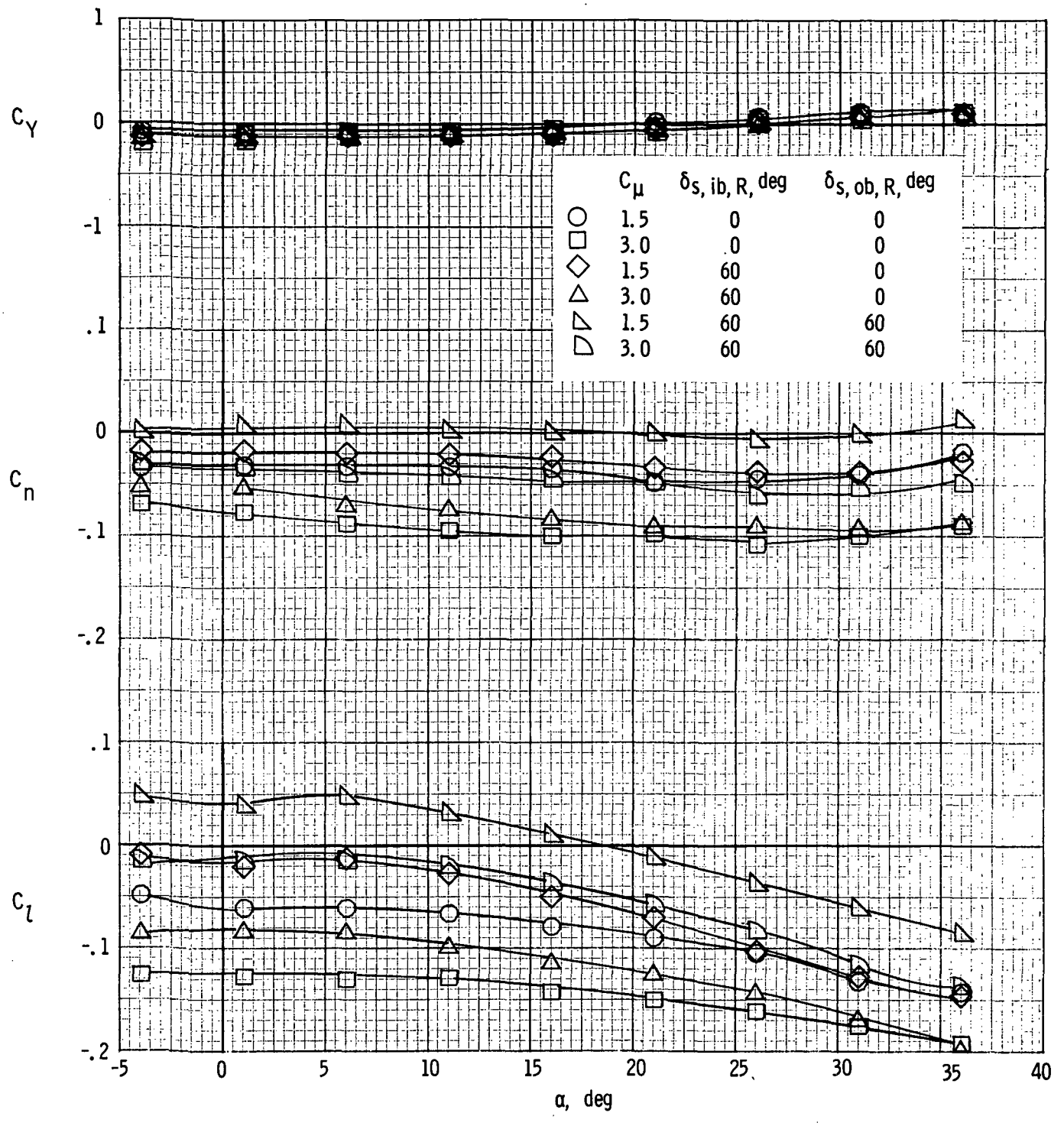

(a) Lateral characteristics.

Figure 10. - Effect of spoiler deflection, left outboard engine not operating, left spoilers not deflected. $\delta_f = 50°$; $i_t = 5°$; $C_{\mu,le} = 0.12$.

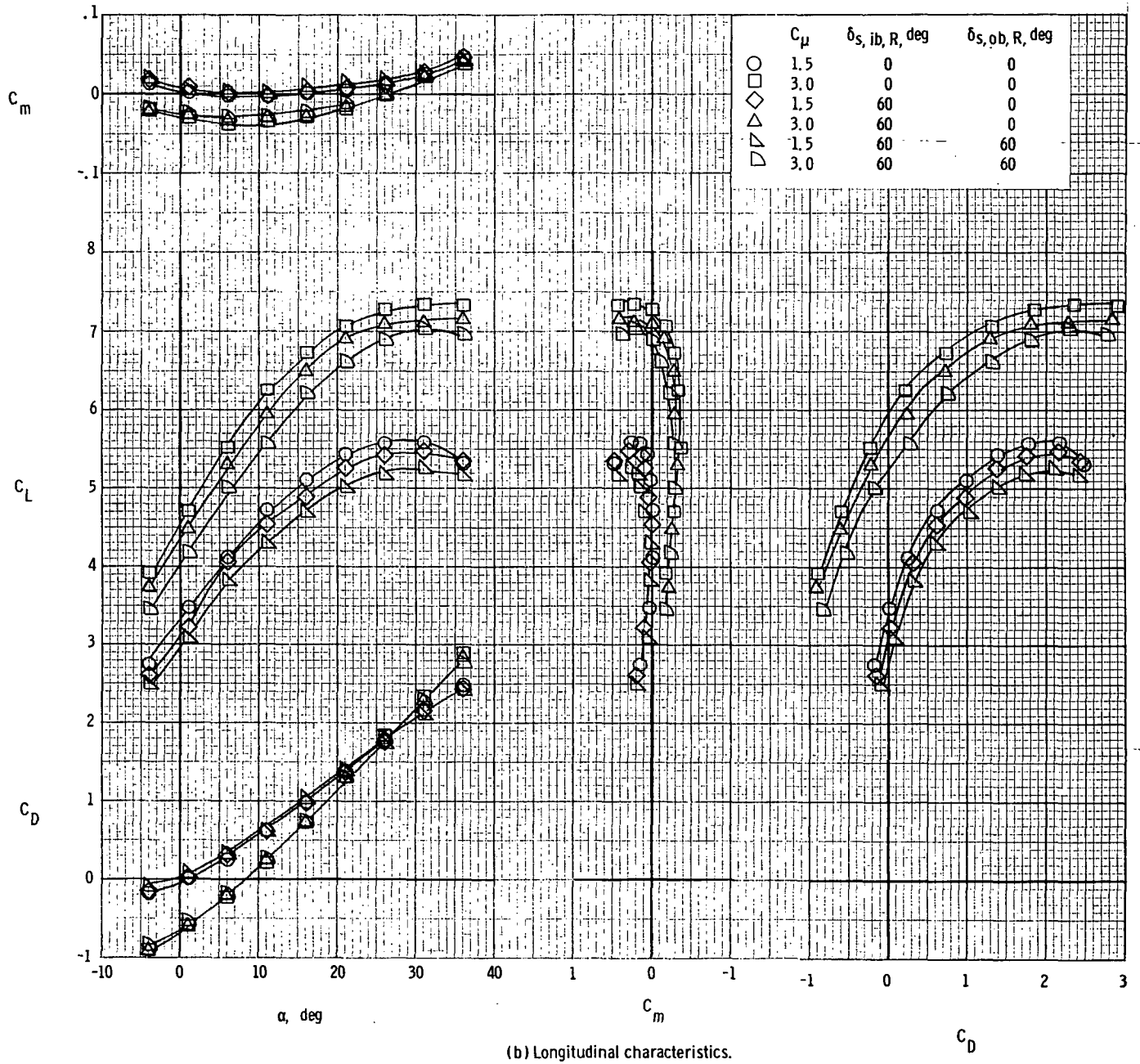

(b) Longitudinal characteristics.

Figure 10. - Concluded.

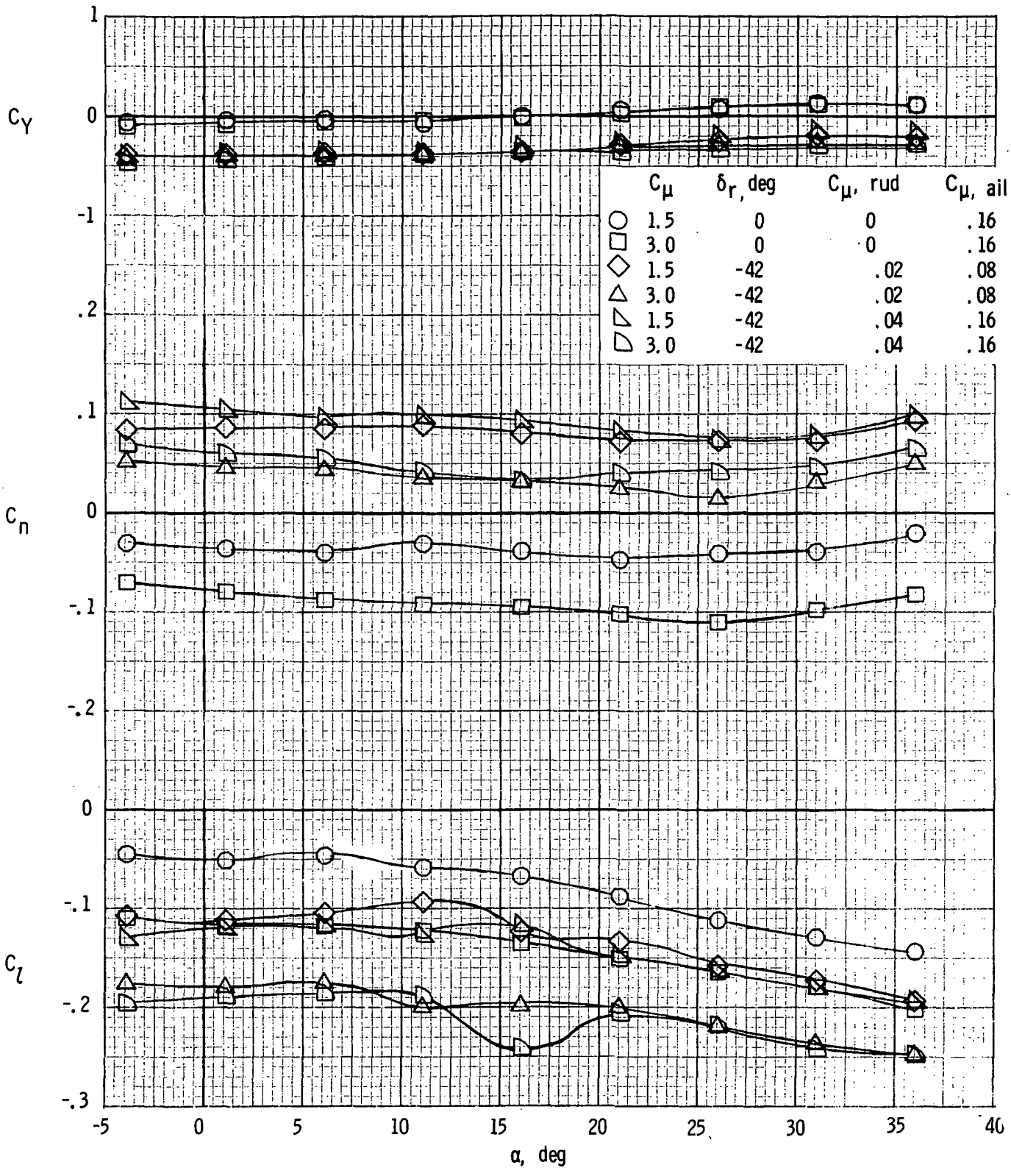

(a) Lateral characteristics.

Figure 11. - Effect of blowing boundary-layer control on rudder, left outboard engine not operating. $\delta_f = 50°$; $i_t = 5°$; C_μ, le = 0.12.

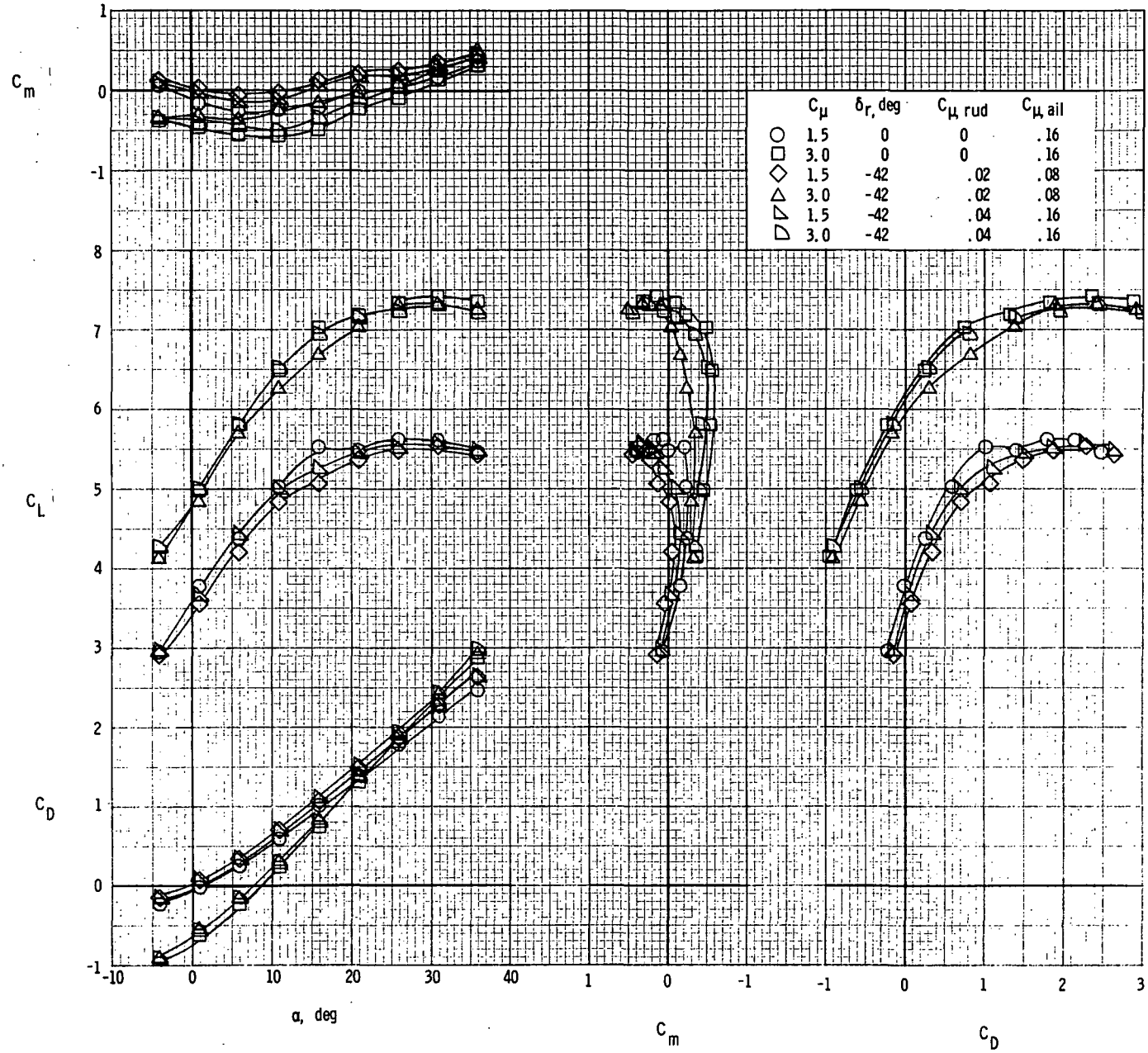

(b) Longitudinal characteristics.

Figure 11. - Concluded.

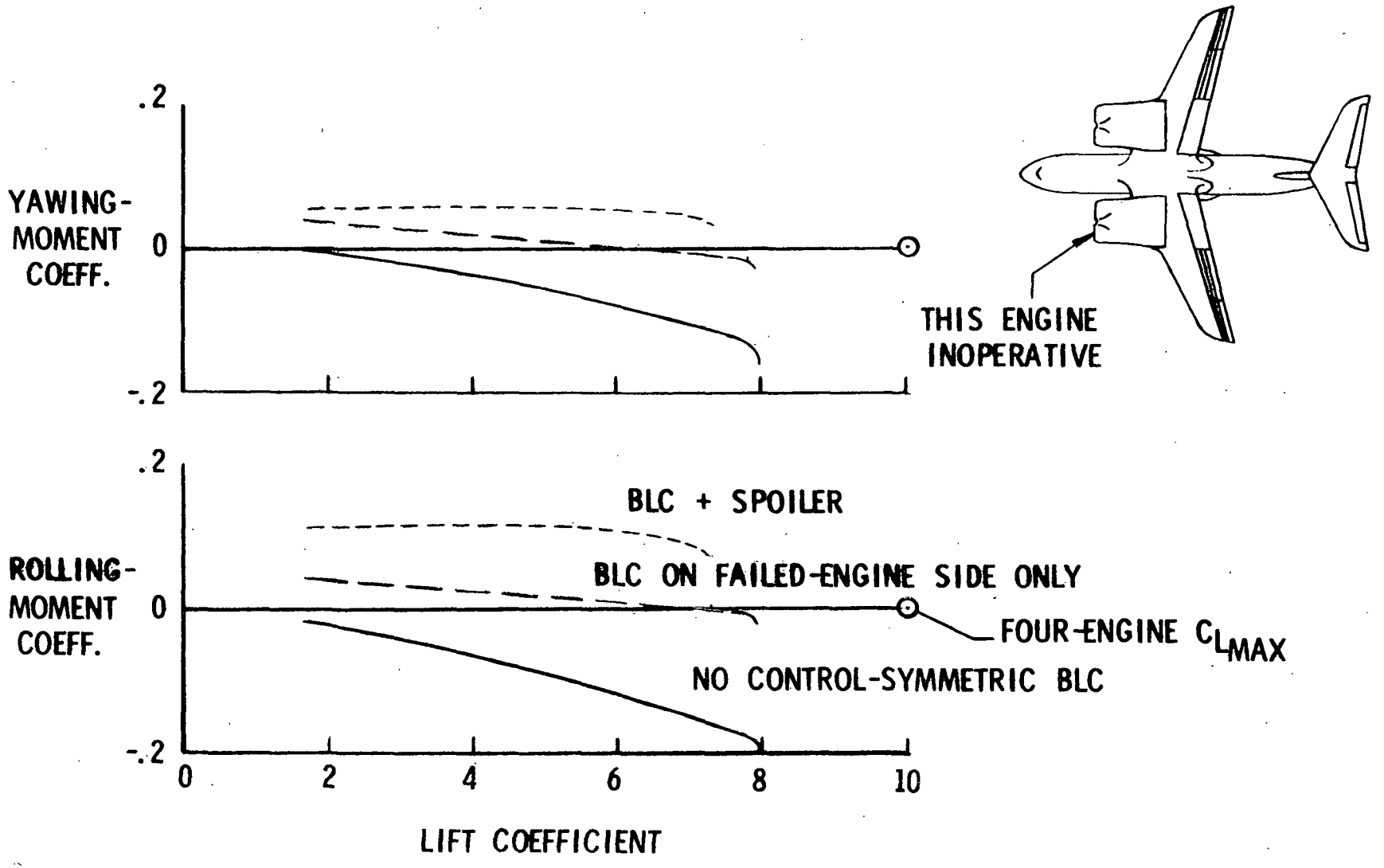

Figure 12. - Lateral trim with asymmetric blowing boundary-layer control on wing leading edge and aileron.